metal-organic compounds

Twinned low-temperature structures of tris(ethylenediamine)zinc(II) sulfate and tris(ethylenediamine)copper(II) sulfate

Martin Lutz

Bijvoet Center for Biomolecular Research, Crystal and Structural Chemistry, Faculty of Science, Utrecht University, Padualaan 8, 3584 CH Utrecht, The Netherlands
Correspondence e-mail: m.lutz@uu.nl

Tris(ethylenediamine)zinc(II) sulfate, $[Zn(C_2H_8N_2)_3]SO_4$, (I), undergoes a reversible solid–solid phase transition during cooling, accompanied by a lowering of the symmetry from high-trigonal $P\bar{3}1c$ to low-trigonal $P\bar{3}$ and by merohedral twinning. The molecular symmetries of the cation and anion change from 32 (D_3) to 3 (C_3). This lower symmetry allows an ordered sulfate anion and generates in the complex cation two independent N atoms with significantly different geometries. The twinning is the same as in the corresponding Ni complex [Jameson *et al.* (1982). *Acta Cryst.* B**38**, 3016–3020]. The low-temperature phase of tris(ethylenediamine)copper(II) sulfate, $[Cu(C_2H_8N_2)_3]SO_4$, (II), has only triclinic symmetry and the unit-cell volume is doubled with respect to the room-temperature structure in $P\bar{3}1c$. (II) was refined as a non-merohedral twin with five twin domains. The asymmetric unit contains two independent formula units, and all cations and anions are located on general positions with 1 (C_1) symmetry. Both molecules of the Cu complex are in elongated octahedral geometries because of the Jahn–Teller effect. This is in contrast to an earlier publication, which describes the complex as a compressed octahedron [Bertini *et al.* (1979). *J. Chem. Soc. Dalton Trans.* pp. 1409–1414].

Comment

We report here the twinned crystal structures of tris(ethylenediamine)zinc(II) sulfate, (I), and tris(ethylenediamine)copper(II) sulfate, (II), both measured at 110 (2) K. At room temperature, the corresponding complexes of vanadium (Daniels *et al.*, 1995), cobalt (Yotnoi *et al.*, 2010), nickel (Mazhar-ul-Haque *et al.*, 1970), copper (Cullen & Lingafelter, 1970) and zinc (Neverov *et al.*, 1990) are isostructural in the trigonal space group $P\bar{3}1c$ and the metal complex is a racemic mixture of the $\delta\delta\delta$ and $\lambda\lambda\lambda$ isomers. There has also been a report of an isostructural manganese complex (Lu, 2009), but because of the positive residual electron density on the site of

the metal and the unusually short metal–nitrogen distance we regard this structure with due care. In $P\bar{3}1c$, the above-mentioned compounds have both the cationic metal complex and the sulfate anion on sites of 32 (D_3) symmetry. The tetrahedral sulfate cannot fulfil this symmetry and must therefore be disordered. Different disorder models have been used in the literature. The octahedral metal complexes can, in principle, have 32 (D_3) symmetry, but in the case of Cu^{2+} with a d^9 electron configuration one would expect different Cu—N distances because of the Jahn–Teller theorem (Procter *et al.*, 1968; Bertini *et al.*, 1977, 1979). Cullen & Lingafelter (1970) describe the presence of dynamic Jahn–Teller effects in the room-temperature structure of the Cu complex with some evidence in the displacement parameters of the N atoms. It is not uncommon to see average structures of Jahn–Teller-distorted complexes in X-ray crystal structure determinations because of the long time scale of the experiment (Persson *et al.*, 2002).

(I) M = Zn
(II) M = Cu
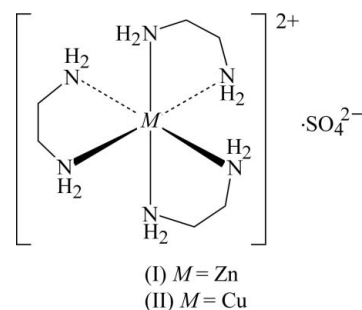
At 110 (2) K, the structure refinement of (I) based on the literature coordinates in space group $P\bar{3}1c$ failed. The $R1$ value remains above 25% and anisotropic refinement leads to nonpositive definite displacement parameters. In the list of the most disagreeable reflections, the values of F_o^2 are significantly larger than F_c^2, which can be considered as a warning sign for twinning (Herbst-Irmer & Sheldrick, 1998). Because splitting of reflections was not detected in the diffraction images, only merohedral twinning is possible. A test with the TWIN-ROTMAT routine of the *PLATON* software (Spek, 2009) did not find suitable twin operations. Therefore, hexagonal twinning of the $P\bar{3}1c$ symmetric structure can be excluded. A closer inspection of the reflections showed that the extinction conditions related to the c-glide plane of $P\bar{3}1c$ are violated. This prompted us to lower the symmetry to space group $P\bar{3}$, which is a maximal isomorphic subgroup. The R_{int} value improves from 0.101 to 0.028 and the $R1$ value improves from 0.265 to 0.183 (isotropic refinement). In the low-trigonal $P\bar{3}$, the twofold rotations perpendicular to the c axis are potential twin operations. A new test with TWINROTMAT now indeed finds the correct twin relation as a twofold rotation about $hkl = (100)$. Its symmetry-equivalent operations can be obtained by a coset decomposition (Flack, 1987) of point group $6/mmm$ with respect to $\bar{3}$ and they are of course also suitable (Table 1). If the correct twin operation is included in the refinement (Herbst-Irmer & Sheldrick, 1998), $R1$ improves to 0.015 and the anisotropic refinement is stable. The twin fraction refined to 0.3745 (9).
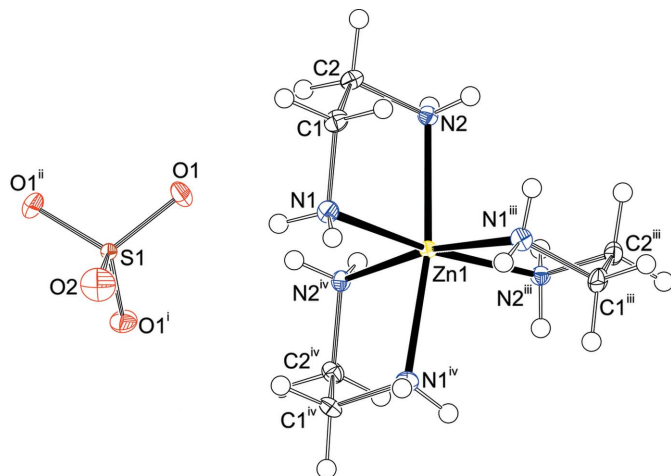
Figure 1
The molecular structure of (I), showing the atom-numbering scheme. Displacement ellipsoids are drawn at the 50% probability level and H atoms are drawn with arbitrary radii. [Symmetry codes: (i) $1 - y, 1 + x - y, z$; (ii) $-x + y, 1 - x, z$; (iii) $1 - y, x - y, z$; (iv) $1 - x + y, 1 - x, z$.]

Figure 2
Schematic representations of the $hk0$ (top) and $hk1$ planes (bottom) based on the A-centred supercell with $V = 5200.7$ (3) $\mathring{A}^3$ (Table 4). The indexing with the supercell (left) predicts too many reflections in $hk0$ and too few in $hk1$. Twinned indexing with three subcells related by 120° rotations about c (right) provides the correct predictions in both planes. Splitting of reflections is ignored in the drawings.

The twinned low-temperature structure of the zinc complex, (I), at 110 (2) K corresponds to the low-temperature structure of the nickel compound in space group $P\bar{3}$ (Jameson *et al.*, 1982), where twinning was also detected. The phase transition of the nickel complex occurs at 180 (1) K (Jameson *et al.*, 1982), while in the zinc complex we still observe $P\bar{3}1c$ symmetry at 140 (2) K during cooling. The phase transition in (I) is reversible and $P\bar{3}1c$ symmetry is regained at 140 (2) K after warming up. In the low-temperature $P\bar{3}$ structure, both the cationic complex and the sulfate anion are located on sites with 3 (C_3) symmetry, which can be fulfilled by the octahedral cation and the tetrahedral anion without disorder (Fig. 1). Because of this symmetry, the zinc complex, (I), has two independent N and C atoms, and the r.m.s. deviation from 32 (D_3) symmetry is 0.0619 Å, as calculated with *MOLSYM* (Pilati & Forni, 1998). Similar to the room-temperature structure, the N—Zn—N angle in the same ethylenediamine ligand ('bite angle') is smaller than 90° and the *trans* angles are smaller than 180°. The Zn1—N2 distance is 0.0311 (15) Å shorter than the Zn1—N1 distance and the C2—N2—Zn1 angle is 1.59 (10)° larger than the corresponding C1—N1—Zn1 angle (Table 2). As Zn^{2+} has a d^{10} electron configuration, electronic reasons can be excluded for this symmetry breaking. It might be a consequence of different inter-molecular hydrogen-bonding geometries: the hydrogen bonds involving N2 are more linear than those involving N1 (Table 3). While the five-membered chelate ring in the room-temperature phase is in an exact C_2 symmetric twist conformation, the ring puckering in (I) is a linear combination of 76.5% of the C_2 symmetric twist and 23.5% of the C_s symmetric envelope conformation (Evans & Boeyens, 1989). The C_2 axis in the room-temperature structure passes through the mid-point of the C—C bond. In (I) at 110 K this mid-point is shifted significantly away from this axis.

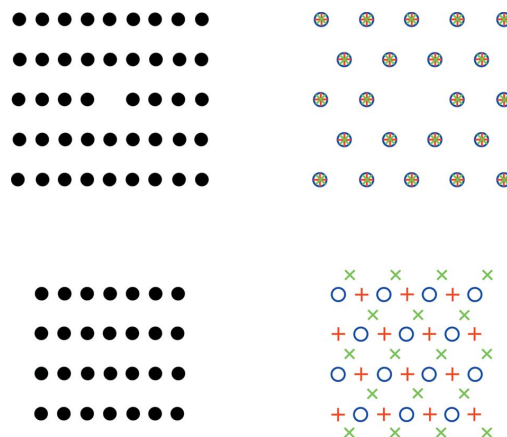The largest change between the room-temperature and the low-temperature phase is in the sulfate anion, which is heavily disordered in $P\bar{3}1c$ and well ordered in $P\bar{3}$. In $P\bar{3}$, one S—O bond of the sulfate tetrahedron is on a threefold axis, while the Zn—N bonds of the $Zn(en)_3$ octahedron (en is ethylenediamine) form angles of 55.28 (3) and 121.00 (3)° with the threefold axis. The ordering of the sulfate now also allows a reliable description of the hydrogen-bonding interactions (Table 3), which was difficult in the room-temperature phase. All four NH hydrogens act as hydrogen-bond donors with sulfate O atoms as acceptors. Each of the two independent O atoms is an acceptor of three hydrogen bonds. Overall, this is an infinite three-dimensional hydrogen-bonding network.

The solid–solid phase transition temperature for the copper complex, (II), is given in the literature as 180 K (Bertini *et al.*, 1977). A low-temperature crystal structure of the copper complex, (II), has been reported (Bertini *et al.*, 1979) based on X-ray data from a diffractometer with a point detector. The authors found a single crystal with unit-cell parameters similar to the trigonal room-temperature cell, but the space-group symmetry was determined as triclinic $P\bar{1}$. The metal complex and the sulfate anion are on general positions (C_1 symmetry) and three sulfate O atoms were refined with a disorder model. The coordination octahedron appeared to be compressed. This is in contrast to a $[Cu(en)_3]Cl_2$ complex described in the same paper, which has the expected elongated octahedra. The sulfate and the chloride complexes have similar g values in low-temperature ESR (electron spin resonance) spectra, which is an indication of a similar geometry of the complexes and contradicts the compression of the octahedron. The presence of three signals in single-crystal ESR spectra would require the presence of three triclinic unit cells, which were not detected in the X-ray diffraction experiment. A contra-diction with the compressed geometry of the Cu complex was later also found with XAFS (X-ray absorption fine structure) (Villain *et al.*, 1997), where equatorial distances of 2.06 and 2.04 Å were determined at room temperature and 10 K, respectively, and axial distances of 2.28 and 2.34 Å.
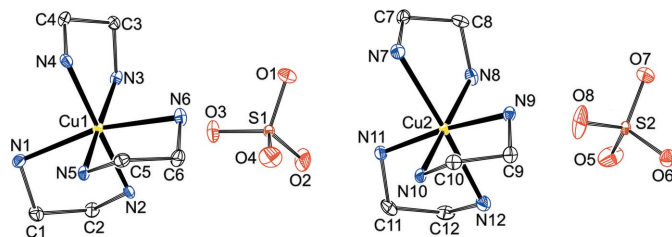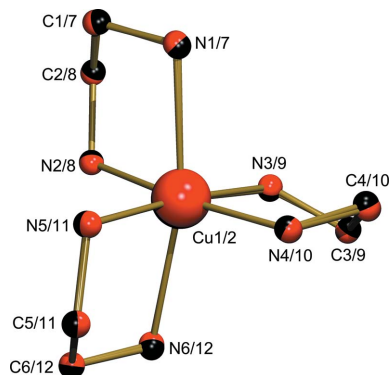
Figure 3
The asymmetric unit of (II), showing the atom-numbering scheme. Displacement ellipsoids are drawn at the 50% probability level and H atoms have been omitted for clarity.

Figure 4
Quaternion fit (Mackay, 1984) of the two independent cations in (II) based on all non-H atoms. The r.m.s. deviation of the fit is 0.041 Å.

In our redetermination of (II) at 110 (2) K, the indexing program *DIRAX* (Duisenberg, 1992) finds a *C*-centred unit cell with $a = 17.6371 (9)$ Å, $b = 30.7843 (12)$ Å, $c = 12.9731 (6)$ Å, $\alpha = 89.976 (2)°$, $\beta = 132.408 (2)°$ and $\gamma = 90.076 (2)°$ (based on 805 reflections between $\theta = 4.12°$ and $\theta = 29.87°$). This cell is a very rough approximation because it ignores the splitting of the reflections. Additionally this cell predicts too many reflections in some reciprocal planes and too few in others (Fig. 2).

To cover all reflections and to take reflection splitting into account, a triclinic subcell must be chosen together with suitable twin operations. The corresponding cell parameters are $a = 8.875$ Å, $b = 12.972$ Å, $c = 13.066$ Å, $\alpha = 71.96°$, $\beta = 70.15°$ and $\gamma = 70.46°$. The volume of this cell is twice the trigonal room-temperature cell. For a better comparison with the room-temperature cell we decided to transform the triclinic *P* cell into a nonstandard triclinic *A* cell (Table 4). Based on this *A*-centred lattice, 120° rotations about the *c* axis are selected as twin operations resulting in three twin domains ('drilling'). This way all reflections are indexed and because of small deviations from exact hexagonal angles the splitting of the reflections can also be explained. Unfortunately, the refinement of the drilling still gives unsatisfactory results. The addition of twofold rotations perpendicular to the *c* axis as twin operations results in six twin domains. The inclusion of the six domains into the refinement improves results, but the twin fraction of one domain remains zero. Therefore the final intensity integration with *EVAL14* (Duisenberg *et al.*, 2003) and the final *SHELXL* (Sheldrick, 2008*b*) refinements are based on five twin domains. The corresponding orientation matrices are given in the CIF file and the refined batch scale factors were 0.402 (3), 0.0191 (7), 0.3395 (18), 0.1480 (18) and 0.0913 (18). A coset decomposition of 6/*mmm* with respect to $\bar{1}$ results in 12 cosets and thus 12 potential twin operations. Only five of these are necessary for a satisfactory refinement.

The asymmetric unit of (II) consists of two independent formula units, and all cations and anions are on general positions with C_1 symmetry (Fig. 3). The two independent cations are related by an approximate threefold rotation about the *c* axis and their geometries are very similar. A quaternion fit (Mackay, 1984) based on all non-H atoms is shown in Fig. 4. Each cation has four short equatorial [2.045 (3)–2.073 (3) Å] and two long axial Cu—N distances [2.373 (3) and 2.396 (4) Å] (Table 5). The equatorial distances are very similar to those in

polymeric $[Cu(SO_4)(C_2H_8N_2)_2]_n$ (Lutz *et al.*, 2010), which has Cu—N distances of 2.0173 (8) and 2.0226 (8) Å. The Jahn–Teller effect, which at room temperature can only be recognized in enlarged anisotropic displacement parameters (Cullen & Lingafelter, 1970), is clearly visible in the different Cu—N bond lengths at 110 (2) K. Here, none of the Cu—N bonds in (II) fails the Hirshfeld rigid bond test (Hirshfeld, 1976) with more than 5σ.

Despite the absence of symmetry, all four equatorial N atoms still form a plane including the Cu atom [the maximal deviation from the least-squares plane is 0.086 (4) Å]. The N—Cu—N bite angles are smaller than the ideal octahedral 90° [79.64 (12)–83.99 (14)°] and the *trans* angles consequently deviate from linearity [166.73 (12)–174.13 (12)°]. The six independent five-membered chelate rings are mainly in the twist conformation. If they are considered as a linear combination of the twist and the envelope conformations, the
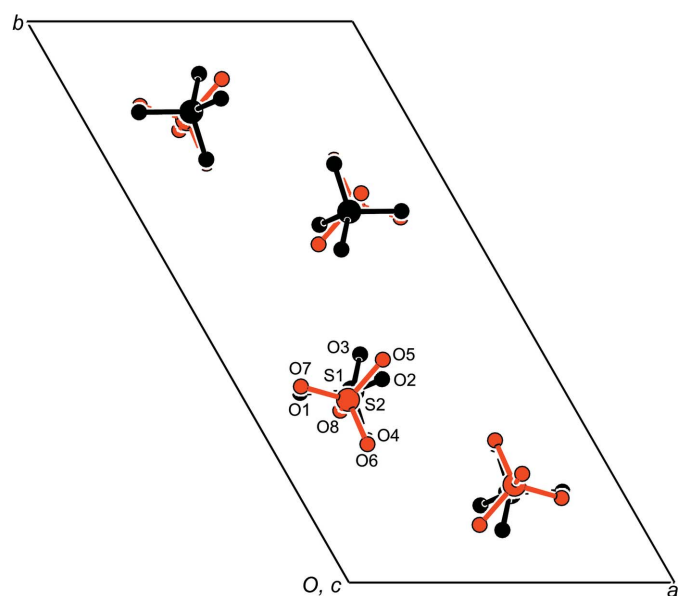
Figure 5
Orientations of the ordered sulfate anions in the unit cell of (II). In the electronic version of the paper, the second residue is drawn in red. The Cu(en)₃ cations are located at the same position in the *a*, *b* direction, but the height in the *c* direction differs by *c*/2.

contribution of the envelope conformation ranges from 0.0 to 37.9%.

In contrast to the room-temperature phase, the two independent sulfate anions in (II) at 110 K are ordered, but have a different orientation with respect to the cell axes (Fig. 5). In fact, the crystal structure has pseudo-translational symmetry, which is only broken by the O atoms of the sulfate. The ADDSYM routine of *PLATON* (Spek, 2009) finds an 83% fit for a halving of the *c* axis. If the O atoms are left out of the analysis, a 100% fit is found. In the standard *P* setting of the space group this would correspond to a pseudo-*I* centring. Despite this pseudosymmetry, no correlation matrix elements for coordinates or displacement parameters are larger than 0.76 in the least-squares refinement. ADDSYM does not indicate the presence of monoclinic or orthorhombic symmetry, while the cell parameters can be transformed to a pseudo-orthorhombic *I* cell with angles close to 90°. Merging of the calculated structure factors according to monoclinic or orthorhombic symmetries results in R_{int} values larger than 0.34.

As the sulfate is ordered in (II), a detailed analysis of the hydrogen bonding is now possible (Table 6). While in the room-temperature phase there are only two independent donor H atoms, (II) at 110 K has 24 independent donor H atoms. There is a large variation in the donor–acceptor distances [between 2.900 (5) and 3.552 (5) Å]. The longest distances belong to the bifurcated hydrogen bonds at H2N and H22N. The hydrogen bonds lead to a densely packed three-dimensional network with a packing index of 76.0% (Kitajgorodskij, 1973).

Experimental

Compounds (I) and (II) were prepared by slowly adding an excess of ethylenediamine at room temperature to a solution of the corresponding metal salt in water. Single crystals were obtained by evaporating the solutions at room temperature.

Compound (I)

Crystal data

[Zn(C₂H₈N₂)₃]SO₄	$Z = 2$
$M_r = 341.74$	Mo $K\alpha$ radiation
Trigonal, $P\bar{3}$	$\mu = 2.03$ mm⁻¹
$a = 8.89410 (11)$ Å	$T = 110$ K
$c = 9.68482 (13)$ Å	$0.30 \times 0.09 \times 0.09$ mm
$V = 663.48 (2)$ Å³	

Data collection

Nonius KappaCCD diffractometer	11327 measured reflections
Absorption correction: analytical	1355 independent reflections
(*SADABS*; Sheldrick, 2008a)	1338 reflections with $I > 2\sigma(I)$
$T_{min} = 0.612$, $T_{max} = 0.872$	$R_{int} = 0.028$

Refinement

$R[F^2 > 2\sigma(F^2)] = 0.015$	H atoms treated by a mixture of
$wR(F^2) = 0.038$	independent and constrained
$S = 1.06$	refinement
1355 reflections	$\Delta\rho_{max} = 0.48$ e Å⁻³
72 parameters	$\Delta\rho_{min} = -0.26$ e Å⁻³

Table 1
Equivalent twin matrices for inclusion in the least-squares refinement of (I).

The matrices were obtained by a coset decomposition (Flack, 1987) of 6/*mmm* with respect to $\bar{3}$ using the Bilbao Crystallographic Server (Aroyo *et al.*, 2006). The twin matrix with respect to (*hkl*) is the transpose of the (*xyz*) matrix of the coordinates.

Twin matrix (*hkl*)	Determinant	Axis
0 $\bar{1}$ 0 / $\bar{1}$ 0 0 / 0 0 $\bar{1}$	+1	2 about (1 $\bar{1}$ 0)
$\bar{1}$ 0 0 / 1 1 0 / 0 0 $\bar{1}$	+1	2 about (0 1 0)
1 1 0 / 0 $\bar{1}$ 0 / 0 0 $\bar{1}$	+1	2 about (1 0 0)
0 1 0 / 1 0 0 / 0 0 1	$\bar{1}$	*m* perpendicular to (1 $\bar{1}$ 0)
1 0 0 / $\bar{1}$ $\bar{1}$ 0 / 0 0 1	$\bar{1}$	*m* perpendicular to (0 1 0)
$\bar{1}$ $\bar{1}$ 0 / 0 1 0 / 0 0 1	$\bar{1}$	*m* perpendicular to (1 0 0)

Table 2
Selected geometric parameters (Å, °) for (I).

Zn1—N1	2.2035 (11)	N2—C2	1.4732 (16)
Zn1—N2	2.1724 (10)	C1—C2	1.5246 (17)
N1—C1	1.4718 (15)		
N1—Zn1—N2	80.66 (4)	C1—N1—Zn1	106.76 (7)
N1—Zn1—N2ⁱ	170.58 (4)	C2—N2—Zn1	108.35 (7)

Symmetry code: (i) $-y + 1, x - y, z$.

Table 3
Hydrogen-bond geometry (Å, °) for (I).

D—H⋯A	D—H	H⋯A	D⋯A	D—H⋯A
N1—H1N⋯O1	0.869 (17)	2.308 (17)	3.0593 (14)	144.8 (14)
N1—H2N⋯O2ⁱⁱ	0.846 (17)	2.220 (17)	2.9711 (16)	148.0 (15)
N2—H3N⋯O1ⁱⁱⁱ	0.824 (17)	2.205 (17)	3.0257 (13)	173.7 (19)
N2—H4N⋯O1ⁱ	0.847 (16)	2.242 (17)	3.0818 (16)	171.5 (15)

Symmetry codes: (i) $-y + 1, x - y, z$; (ii) $-x + 1, -y + 1, -z$; (iii) $y, -x + y, -z + 1$.

Compound (II)

Crystal data

[Cu(C₂H₈N₂)₃]SO₄	$\gamma = 119.845 (4)°$
$M_r = 339.91$	$V = 2600.5 (3)$ Å³
Triclinic, $A\bar{1}$	$Z = 8$
$a = 8.8749 (7)$ Å	Mo $K\alpha$ radiation
$b = 17.6358 (11)$ Å	$\mu = 1.86$ mm⁻¹
$c = 19.1559 (11)$ Å	$T = 110$ K
$\alpha = 89.582 (3)°$	$0.33 \times 0.15 \times 0.06$ mm
$\beta = 90.296 (5)°$	

Data collection

Nonius KappaCCD diffractometer	18964 measured reflections
Absorption correction: multi-scan	5825 independent reflections
(*TWINABS*; Sheldrick, 2008a)	4478 reflections with $I > 2\sigma(I)$
$T_{min} = 0.60$, $T_{max} = 0.75$	$R_{int} = 0.033$

Refinement

$R[F^2 > 2\sigma(F^2)] = 0.033$	329 parameters
$wR(F^2) = 0.076$	H-atom parameters constrained
$S = 1.02$	$\Delta\rho_{max} = 0.77$ e Å⁻³
5825 reflections	$\Delta\rho_{min} = -0.63$ e Å⁻³

Compound (I) was measured with a detector distance of 40 mm, a scan angle of 1° and an exposure time of 15 seconds per frame; 652

metal-organic compounds

Table 4
Relationship between the trigonal room-temperature cell of (II) (Cullen & Lingafelter, 1970) and the different possibilities of indexing the triclinic structure at 110 K.

	Room temperature	Approximate supercell at 110 K	True cell at 110 K
Nonstandard setting	Bravais = P $a = 8.966$ (1) Å $b = 8.966$ (1) Å $c = 9.597$ (1) Å $\alpha = 90°$ $\beta = 90°$ $\gamma = 120°$ $V = 668.13$ (13) Å^3	Bravais = A $a = 17.7495$ (6) Å $b = 17.6371$ (9) Å $c = 19.1581$ (10) Å $\alpha = 89.585$ (4)° $\beta = 90.239$ (3)° $\gamma = 119.687$ (2)° $V = 5200.7$ (3) Å^3	Bravais = A $a = 8.8749$ (7) Å $b = 17.6358$ (11) Å $c = 19.1559$ (11) Å $\alpha = 89.582$ (3)° $\beta = 90.296$ (5)° $\gamma = 119.845$ (4)° $V = 2600.5$ (3) Å^3
Standard setting	Bravais = P $a = 8.966$ (1) Å $b = 8.966$ (1) Å $c = 9.597$ (1) Å $\alpha = 90°$ $\beta = 90°$ $\gamma = 120°$ $V = 668.13$ (13) Å^3	Bravais = C $a = 17.6371$ (9) Å $b = 30.7843$ (12) Å $c = 12.9731$ (6) Å $\alpha = 89.976$ (2)° $\beta = 132.408$ (2)° $\gamma = 90.076$ (2)° $V = 5200.7$ (3) Å^3	Bravais = P $a = 8.8749$ (7) Å $b = 12.9715$ (6) Å $c = 13.0660$ (9) Å $\alpha = 71.959$ (5)° $\beta = 70.148$ (5)° $\gamma = 70.459$ (5)° $V = 1300.25$ (16) Å^3
Reduced setting	Bravais = P $a = 8.966$ (1) Å $b = 8.966$ (1) Å $c = 9.597$ (1) Å $\alpha = 90°$ $\beta = 90°$ $\gamma = 120°$ $V = 668.13$ (13) Å^3	Bravais = P $a = 12.9731$ (6) Å $b = 13.0671$ (8) Å $c = 17.7292$ (6) Å $\alpha = 109.702$ (4)° $\beta = 109.578$ (2)° $\gamma = 94.735$ (4)° $V = 2600.4$ (2) Å^3	Bravais = P $a = 8.8749$ (7) Å $b = 12.9715$ (6) Å $c = 13.0660$ (9) Å $\alpha = 71.959$ (5)° $\beta = 70.148$ (5)° $\gamma = 70.459$ (5)° $V = 1300.25$ (16) Å^3

Table 5
Selected geometric parameters (Å, °) for (II).

Cu1—N1	2.395 (3)	Cu2—N7	2.373 (3)
Cu1—N2	2.063 (3)	Cu2—N8	2.045 (3)
Cu1—N3	2.048 (3)	Cu2—N9	2.049 (3)
Cu1—N4	2.055 (3)	Cu2—N10	2.052 (3)
Cu1—N5	2.052 (3)	Cu2—N11	2.073 (3)
Cu1—N6	2.375 (3)	Cu2—N12	2.396 (4)
N1—Cu1—N6	166.73 (12)	N7—Cu2—N12	167.91 (13)
N2—Cu1—N4	173.29 (14)	N8—Cu2—N10	173.49 (15)
N3—Cu1—N5	174.13 (12)	N9—Cu2—N11	173.57 (13)

Table 6
Hydrogen-bond geometry (Å, °) for (II).

D—H$\cdots A$	D—H	H$\cdots A$	$D\cdots A$	D—H$\cdots A$
N1—H1N$\cdots$O5^{i}	0.92	2.27	3.180 (5)	172
N1—H2N$\cdots$O5^{ii}	0.92	2.52	3.358 (5)	151
N1—H2N$\cdots$O7^{ii}	0.92	2.50	3.267 (5)	141
N2—H3N$\cdots$O3	0.92	2.12	2.993 (4)	157
N2—H4N$\cdots$O4^{iii}	0.92	2.05	2.914 (4)	156
N3—H5N$\cdots$O3	0.92	2.08	2.954 (4)	158
N3—H6N$\cdots$O5^{ii}	0.92	2.06	2.920 (4)	155
N4—H7N$\cdots$O7^{i}	0.92	2.07	2.982 (4)	174
N4—H8N$\cdots$O1^{iv}	0.92	2.13	3.040 (4)	172
N5—H9N$\cdots$O6^{i}	0.92	2.03	2.947 (4)	173
N5—H10N$\cdots$O2^{iii}	0.92	2.37	3.119 (5)	139
N6—H11N$\cdots$O4	0.92	2.19	3.089 (5)	166
N6—H12N$\cdots$O1^{iv}	0.92	2.30	3.070 (5)	141
N7—H13N$\cdots$O1	0.92	2.27	3.146 (5)	160
N7—H14N$\cdots$O7^{v}	0.92	2.45	3.312 (5)	156
N8—H15N$\cdots$O8	0.92	2.14	2.975 (5)	151
N8—H16N$\cdots$O3^{ii}	0.92	2.00	2.914 (4)	172
N9—H17N$\cdots$O8	0.92	2.06	2.907 (5)	152
N9—H18N$\cdots$O7^{v}	0.92	2.30	3.109 (5)	146
N10—H19N$\cdots$O2	0.92	2.25	3.056 (4)	147
N10—H20N$\cdots$O6^{vi}	0.92	2.17	3.079 (5)	172
N11—H21N$\cdots$O2	0.92	2.03	2.900 (5)	158
N11—H22N$\cdots$O2^{ii}	0.92	2.67	3.552 (5)	161
N11—H22N$\cdots$O3^{ii}	0.92	2.66	3.458 (5)	145
N12—H23N$\cdots$O8	0.92	2.46	3.177 (5)	135
N12—H24N$\cdots$O6^{vi}	0.92	2.53	3.268 (5)	137

Symmetry codes: (i) $x, y, z - 1$; (ii) $-x + 1, -y + 1, -z + 1$; (iii) $-x + 1, -y + \frac{1}{2}, -z + \frac{1}{2}$; (iv) $-x, -y + \frac{1}{2}, -z + \frac{1}{2}$; (v) $-x, -y + \frac{1}{2}, -z + \frac{3}{2}$; (vi) $-x + 1, -y + \frac{1}{2}, -z + \frac{3}{2}$.

frames were collected. The intensity data of (I) were obtained using a single orientation matrix. For the refinement, a TWIN and a BASF instruction (*SHELXL97*; Sheldrick, 2008*b*) were included. All H atoms were located in difference Fourier maps and refined freely with isotropic displacement parameters.

Compound (II) was measured with a detector distance of 50 mm, a scan angle of 0.5° and an exposure time of 20 seconds per frame; 1615 frames were collected. The intensity data of (II) were obtained using five orientation matrices. Only the single non-overlapping reflections of the major domain and the overlapping reflections with the major domain were taken into account. These data were merged prior to the refinement using the *TWINABS* software (Sheldrick, 2008*a*), resulting in an HKLF-5 type of reflection file (Herbst-Irmer & Sheldrick, 1998). H atoms were included in calculated positions and refined using a riding model, with C—H = 0.99 Å and N—H = 0.92 Å, and with U_{iso}(H) = $1.2U_{iso}$(C,N).

For both compounds, data collection: *COLLECT* (Nonius, 1999); cell refinement: *PEAKREF* (Schreurs, 2005). Data reduction: *EVAL15* (Schreurs *et al.*, 2010) and *SADABS* (Sheldrick, 2008*a*) for (I); *EVAL14* (Duisenberg *et al.*, 2003) and *TWINABS* (Sheldrick, 2008*a*) for (II). For both compounds, program(s) used to solve structure: *SHELXS97* (Sheldrick, 2008*b*); program(s) used to refine structure: *SHELXL97* (Sheldrick, 2008*b*); molecular graphics: *PLATON* (Spek, 2009); software used to prepare material for publication: manual editing of the *SHELXL* CIF file.

References

Aroyo, M. I., Perez-Mato, J. M., Capillas, C., Kroumova, E., Ivantchev, S., Madariaga, G., Kirov, A. & Wondratschek, H. (2006). *Z. Kristallogr.* **221**, 15–27.
Bertini, I., Dapporto, P., Gatteschi, D. & Scozzafava, A. (1979). *J. Chem. Soc. Dalton Trans.* pp. 1409–1414.
Bertini, I., Gatteschi, D. & Scozzafava, A. (1977). *Inorg. Chem.* **16**, 1973–1976.
Cullen, D. L. & Lingafelter, E. C. (1970). *Inorg. Chem.* **9**, 1858–1864.
Daniels, L. M., Murillo, C. A. & Rodriguez, K. G. (1995). *Inorg. Chim. Acta*, **229**, 27–32.
Duisenberg, A. J. M. (1992). *J. Appl. Cryst.* **25**, 92–96.
Duisenberg, A. J. M., Kroon-Batenburg, L. M. J. & Schreurs, A. M. M. (2003). *J. Appl. Cryst.* **36**, 220–229.
Evans, D. G. & Boeyens, J. C. A. (1989). *Acta Cryst.* B**45**, 581–590.
Flack, H. D. (1987). *Acta Cryst.* A**43**, 564–568.
Herbst-Irmer, R. & Sheldrick, G. M. (1998). *Acta Cryst.* B**54**, 443–449.
Hirshfeld, F. L. (1976). *Acta Cryst.* A**32**, 239–244.
Jameson, G. B., Schneider, R., Dubler, E. & Oswald, H. R. (1982). *Acta Cryst.* B**38**, 3016–3020.
Kitajgorodskij, A. I. (1973). In *Molecular Crystals and Molecules*. New York: Academic Press.
Lu, J. (2009). *Acta Cryst.* E**65**, m1187.
Lutz, M., Smeets, S. & Parois, P. (2010). *Acta Cryst.* E**66**, m671–m672.

Mackay, A. L. (1984). *Acta Cryst.* A**40**, 165–166.

Mazhar-ul-Haque, Caughlan, C. N. & Emerson, K. (1970). *Inorg. Chem.* **9**, 2421–2424.

Neverov, V. A., Mazus, M. D., Biyushkin, V. N. & Malinovskii, T. I. (1990). *Kristallografiya*, **35**, 1281–1283.

Nonius (1999). *COLLECT*. Nonius BV, Delft, The Netherlands.

Persson, I., Persson, P., Sandström, M. & Ullström, A.-S. (2002). *J. Chem. Soc. Dalton Trans.* pp. 1256–1265.

Pilati, T. & Forni, A. (1998). *J. Appl. Cryst.* **31**, 503–504.

Procter, I. M., Hathaway, B. J. & Nicholls, P. (1968). *J. Chem. Soc. A*, pp. 1678–1684.

Schreurs, A. M. M. (2005). *PEAKREF*. Utrecht University, The Netherlands.

Schreurs, A. M. M., Xian, X. & Kroon-Batenburg, L. M. J. (2010). *J. Appl. Cryst.* **43**, 70–82.

Sheldrick, G. M. (2008a). *SADABS* (Version 2008/1) and *TWINABS* (Version 2008/4). University of Göttingen, Germany.

Sheldrick, G. M. (2008b). *Acta Cryst.* A**64**, 112–122.

Spek, A. L. (2009). *Acta Cryst.* D**65**, 148–155.

Villain, F., Verdaguer, M. & Dromzee, Y. (1997). *J. Phys. IV Fr.* **7**, C2-659–C2-660.

Yotnoi, B., Seeharaj, A., Chimupala, Y. & Rujiwatra, A. (2010). *Acta Cryst.* E**66**, m628.